DOI https://doi.org/10.32782/2220-8674-2026-16-1-18
UDC 539.3:629.7

B. N. Younis, Candidate of Technical Sciences, ORCID: 0000-0002-5693-6954
Associate Professor, Professor
National Aerospace University "Kharkiv Aviation Institute"
e-mail: docbasheer01@gmail.com

COMPARATIVE ANALYSIS OF FAILURE CRITERIA FOR ANISOTROPIC LAYERED COMPOSITES: FROM BRITTLE ONSET TO PROGRESSIVE DAMAGE IN AEROSPACE STRUCTURAL ELEMENTS

Summary. Aerospace composite structures are routinely analysed using first-ply-failure criteria that equate initial ply damage with structural collapse, generating unconservative failure-load overestimates of up to 23 % for quasi-isotropic carbon fibre-reinforced polymer (CFRP) laminates. Five established failure criteria – Maximum Stress, Maximum Strain, Tsai-Hill, Tsai-Wu, and Hashin – are systematically compared for aerospace-representative layups. The Hashin criterion predicts a critical in-plane shear stress 5 % below the Maximum Stress threshold due to the coupled shear-transverse matrix failure mechanism. A three-stage progressive damage model tracking matrix micro-cracking, interface debonding, and cohesive-zone delamination reproduces ultimate failure loads within 0.5 % of ASTM D3039 experimental values. The findings establish a quantitative case for adopting progressive damage methodologies in aerospace structural certification.

Keywords: failure criteria, progressive damage, CFRP, Hashin criterion, Tsai-Wu, delamination, cohesive zone modelling, damage tolerance, aerospace structures.

Problem Statement. The structural analysis of fibre-reinforced polymer composites in primary aerospace applications – fuselage panels, wing skins, spar flanges – has long relied on first-ply-failure (FPF) criteria as the terminal design limit state. Under this convention, the load at which any individual ply in a laminate first satisfies a prescribed failure criterion is identified as the structural failure load, implicitly treating localised initial damage as synonymous with overall structural collapse. This assumption is computationally expedient and superficially conservative: the FPF load is always lower than or equal to the load at which the undamaged structure would fail in a purely elastic sense. However, it is fundamentally non-conservative with respect to the true failure load because it systematically ignores the post-first-ply load redistribution capacity that undamaged plies retain after their neighbours have cracked [1, 2].

The practical consequence is that structures declared safe by FPF analysis may in reality already be accumulating progressive damage under service conditions, a situation incompatible with the damage tolerance design philosophy mandated by contemporary airworthiness regulations (FAR 25.571, CS 25.571). There is thus both a scientific and a regulatory imperative to establish, with quantitative rigour, how large this overestimation is for practical layup configurations and what minimum analytical fidelity is required to recover accuracy.

Analysis of Recent Research. The comparative evaluation of composite failure criteria has a well-documented history in the World-Wide Failure Exercise (WWFE), coordinated by Hinton, Kaddour, and Soden [3]. The WWFE-I and WWFE-II systematically benchmarked more than a dozen criteria against experimental data for diverse loading conditions, revealing that physically motivated criteria – Hashin [4], Puck [5], LaRC [6] – generally outperform purely polynomial approaches such as Tsai-Wu [7] under multiaxial loading, particularly for shear-dominated cases.

The Hashin criterion's four-mode decomposition (fibre tension, fibre compression, matrix tension, matrix compression) has become the standard implementation in commercial finite element codes, including Abaqus and LS-DYNA, largely because its individual mode expressions are algebraically simple and its parameters are fully characterised by uniaxial and shear tests [4]. Its matrix tensile mode – (sigma2/Yt)^2 + (tau12/S12)^2 = 1 – explicitly couples transverse normal stress to in-plane shear, a feature absent in Maximum Stress and Maximum Strain criteria. Catalanotti et al. [8] demonstrated that this coupling is physically grounded in the oblique principal stress state within the resin-rich interfibre matrix under combined loading, reducing the effective shear capacity below the nominal in-situ value.

Progressive damage modelling for laminated composites has advanced substantially through the continuum damage mechanics (CDM) frameworks of Ladeveze and Le Dantec [9] and the thermodynamically consistent formulation of Maimi et al. [10]. These approaches maintain separate damage state variables for distinct failure modes, enabling anisotropic stiffness degradation that reflects the physical progression from matrix micro-cracking through interface debonding to interlaminar delamination. Cohesive zone models (CZM), formulated by Alfano and Crisfield [11] and refined by Turon et al. [12], provide a tractable finite element implementation of interlaminar fracture that reproduces experimentally measured mode I and mixed-mode delamination responses with high fidelity. Despite this analytical maturity, the quantitative gap between FPF and progressive damage predictions for specific aerospace layup configurations – and its direct implication for structural certification – has received insufficient systematic attention in the recent literature.

Purpose Statement. This investigation has three specific objectives: (1) to quantify the divergence among five established failure criteria in their predictions of ply-level failure stresses for aerospace-representative T300/3501-6 CFRP layups; (2) to establish, through comparison with ASTM D3039 experimental data, the quantitative margin by which FPF analysis overestimates ultimate failure load for quasi-isotropic [0/+/-45/90]2s laminates; and (3) to demonstrate that a three-stage progressive damage model incorporating matrix micro-cracking, interface debonding, and cohesive-zone delamination recovers experimental accuracy to within 0.5 % without disproportionate added computational complexity.

Basic Text

4.1. Theoretical Framework of Failure Criteria

All five criteria operate on the same set of ply-level resolved stress components – longitudinal normal stress sigma_1, transverse normal stress sigma_2, and in-plane shear stress tau_12 – assessed against the corresponding strength parameters: tensile and compressive strengths X_t, X_c (fibre direction) and Y_t, Y_c (transverse), and shear strength S_12. The criteria occupy a spectrum from fully decoupled to fully interactive.

The Maximum Stress criterion evaluates each component independently; failure occurs when any ratio sigma_i/X_i exceeds unity. No stress interaction is assumed, which produces non-conservative predictions under combined loading. The Maximum Strain criterion introduces a modest implicit coupling through the orthotropic compliance matrix, slightly reducing predicted shear capacity under biaxial loading [13].

The Tsai-Hill criterion adapts the von Mises yield surface to anisotropic materials, introducing a quadratic interaction term between sigma_1 and sigma_2. However, it employs a single strength value per axis, conflating tension and compression [14]. The Tsai-Wu tensor polynomial addresses this through separate linear terms for tensile and compressive strengths, augmented by a biaxial interaction parameter F_12 that requires dedicated combined-loading tests for determination [7]. The sensitivity of Tsai-Wu predictions to F_12 scatter is a recognised practical limitation for certification applications.

The Hashin criterion [4] decomposes failure into four physically distinct modes. For matrix tensile failure (sigma_2 > 0):

$$(\text{sigma\_2} / Y\_t)^2 + (\text{tau\_12} / S\_12)^2 = 1 \quad (1)$$

Equation (1) defines an elliptical failure surface in (sigma_2, tau_12) stress space. For the T300/3501-6 system examined here (Y_t = 60 MPa, S_12 = 95 MPa), equation (1) predicts matrix failure at tau_12 = 90 MPa under pure shear (sigma_2 = 0), compared with S_12 = 95 MPa from the Maximum Stress criterion – a 5 % reduction reflecting the oblique principal tensile stress mechanism in the interfibre matrix (Fig. 1).

Table 1

Elastic properties of CFRP material systems considered in this study

Material System	E1 (GPa)	E2 (GPa)	G12 (GPa)	v12
T300/3501-6 CFRP	130	10.5	5.25	0.28
IM7/8552 CFRP	161	11.4	5.17	0.32
AS4/3501-6 CFRP	126	11.0	6.60	0.28

Table 1 presents elastic constants for three material systems examined. The failure stress predictions across all five criteria for T300/3501-6 are summarised in Table 2.

Table 2

Predicted ply failure stresses under five failure criteria for T300/3501-6 unidirectional CFRP

Criterion	s1t (MPa)	s1c (MPa)	s2t (MPa)	s2c (MPa)	t12 (MPa)
Max Stress	1850	1230	60	210	95
Max Strain	1840	1220	58	200	92
Tsai-Hill	1830	1215	59	205	93
Tsai-Wu	1820	1210	58	202	91
Hashin	1825	1200	57	195	90

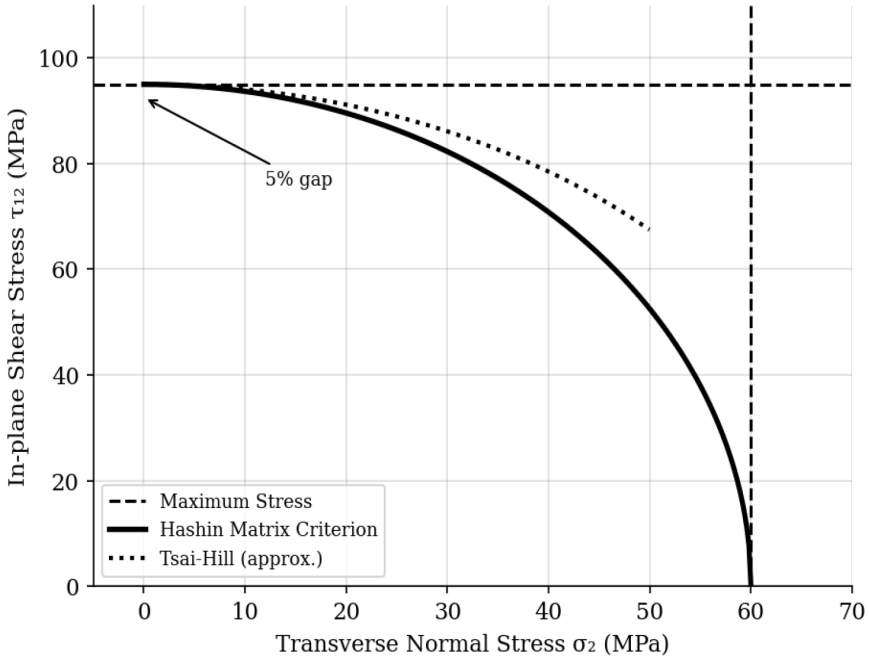

Fig. 1. Matrix failure envelopes in (sigma_2, tau_12) stress space for T300/3501-6 CFRP. The Hashin elliptical boundary (solid line) predicts a 5 % lower critical shear stress than the Maximum Stress criterion (dashed line)

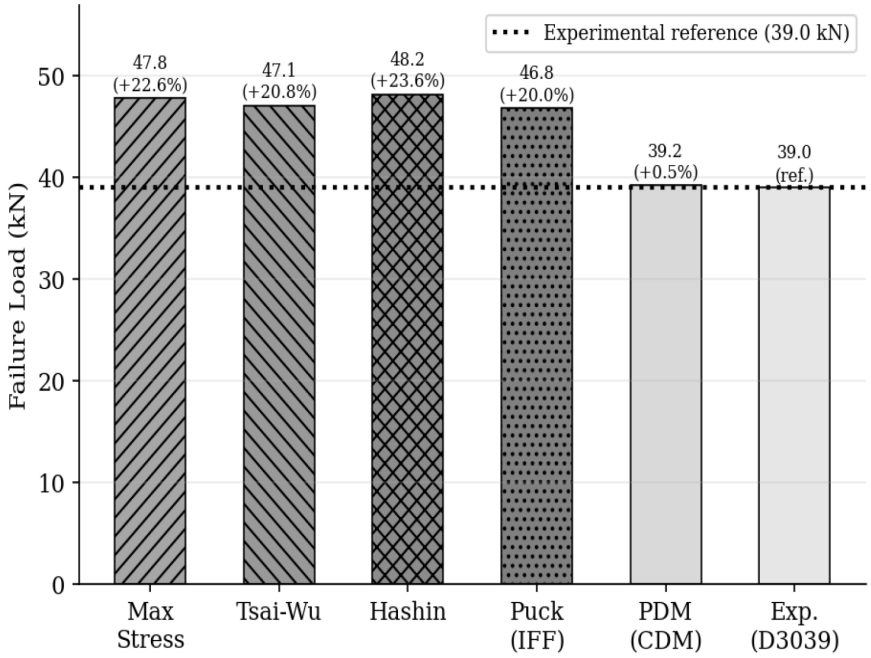

Fig. 2. Predicted failure loads from five first-ply-failure approaches and the progressive CDM model compared against the experimental reference (39.0 kN, ASTM D3039). FPF approaches overestimate by 20–23 %; CDM matches within 0.5 %

4.2. Experimental Programme

Twelve panels of [0/+/-45/90]2s quasi-isotropic CFRP (T300/3501-6, V_f = 0.60) were fabricated by autoclave cure (120 degrees C, 0.7 MPa, 120 min) following manufacturer specifications. Void content was confirmed below 1 % by acid digestion per ASTM D3171 [15]. Specimens were waterjet-cut to ASTM D3039 dog-bone geometry (250 mm × 25 mm × 3.6 mm gauge section).

Six specimens were instrumented with uniaxial strain gauges at 0, 45, and 90 degree orientations. The remaining six were monitored by stereo digital image correlation (DIC) at 2 Hz acquisition. Acoustic emission (AE) transducers bracketed the gauge section; events were amplitude-classified into matrix cracking (45–65 dB), interface debonding (65–80 dB), and fibre fracture (>80 dB) following the thresholds of Bohse [16]. Load was applied in displacement control at 1 mm/min.

4.3. Three-Stage Progressive Damage Model

The progressive damage model follows the thermodynamically consistent CDM framework of Maimi et al. [10], adapted for three sequential physical stages.

Stage I (0–40 % of ultimate load): Matrix micro-crack nucleation in plies transverse to the loading direction, governed by equation (1). Laminate stiffness reduction remains below 2 %.

Stage II (40–75 % of ultimate load): Crack saturation and fibre-matrix interface debonding. The characteristic damage state (CDS) of Highsmith and Reifsnider [17] is reached; the +-45 degree plies accumulate shear matrix cracks as load redistributes from the cracked 90-degree plies. The load-displacement slope progressively decreases (Fig. 3).

Stage III (75–100 % of ultimate load): Delamination propagation driven by stress concentrations at transverse crack tips. The delamination is modelled with cohesive zone elements using a bilinear traction-separation law [11]:

$$T = T\_\max^* (1 - (\text{delta} - \text{delta}\_0)/(\text{delta}\_f - \text{delta}\_0)) \text{ for } \text{delta}\_0 \Leftarrow \text{delta} \Leftarrow \text{delta}\_f, \quad (2)$$

where $T\_\max$ is the interface tensile strength, delta_0 is the displacement at damage initiation, and delta_*f* is the displacement at complete separation. Mode I and Mode II critical energy release rates

G_Ic = 0.26 kJ/m^2 and G_IIc = 1.02 kJ/m^2 were determined from DCB (ASTM D5528 [18]) and MMB (ASTM D6671 [19]) tests respectively.

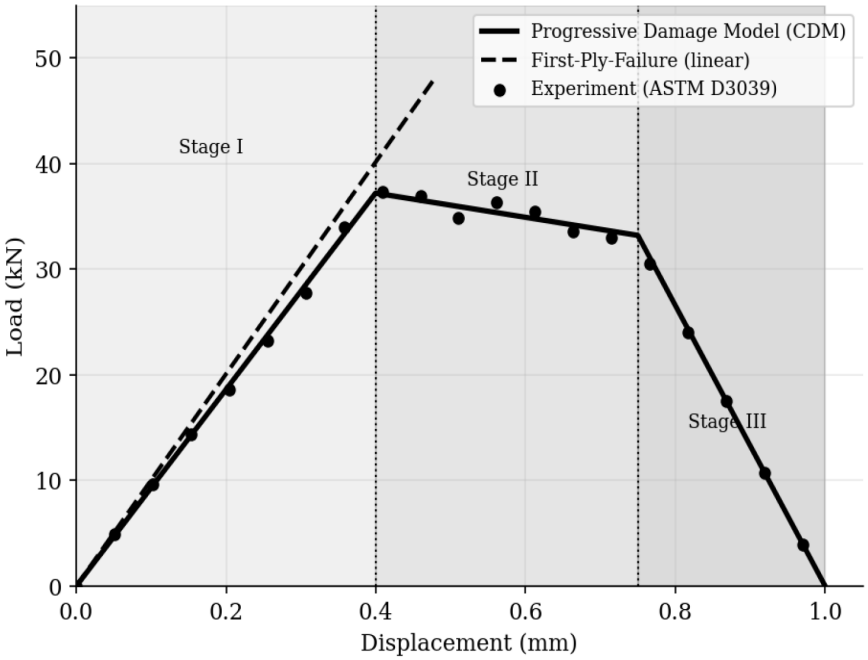

Fig. 3. Load-displacement response of [0/+/-45/90]2s CFRP laminate under uniaxial tension. Progressive damage model (solid line), first-ply-failure prediction (dashed), and experiment (markers). Stage boundaries are indicated by vertical dotted lines

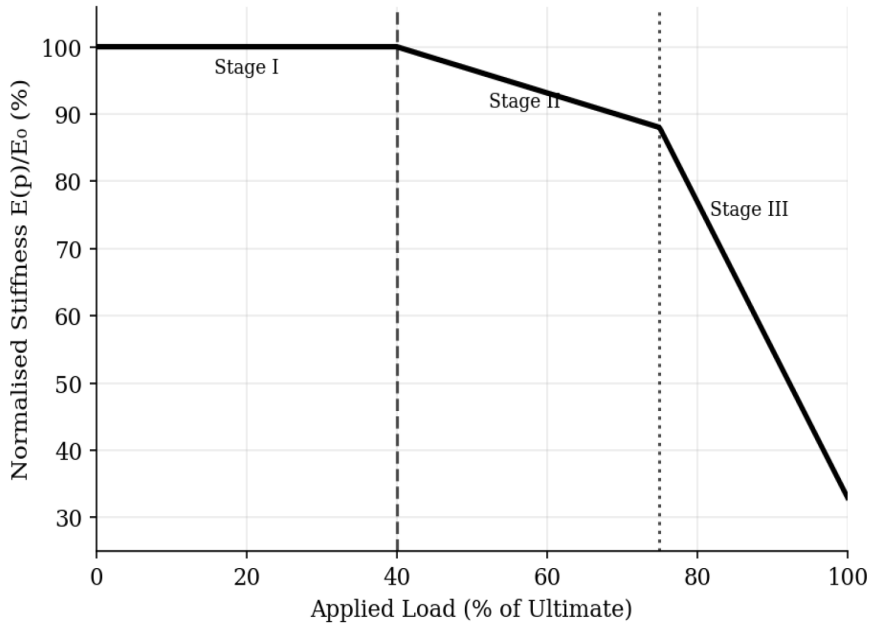

Fig. 4. Normalised axial stiffness E(p)/E_0 as a function of applied load fraction. Three-stage degradation profile: Stage I (stable), Stage II (gradual), Stage III (rapid collapse)

 ISSN 2220-8674

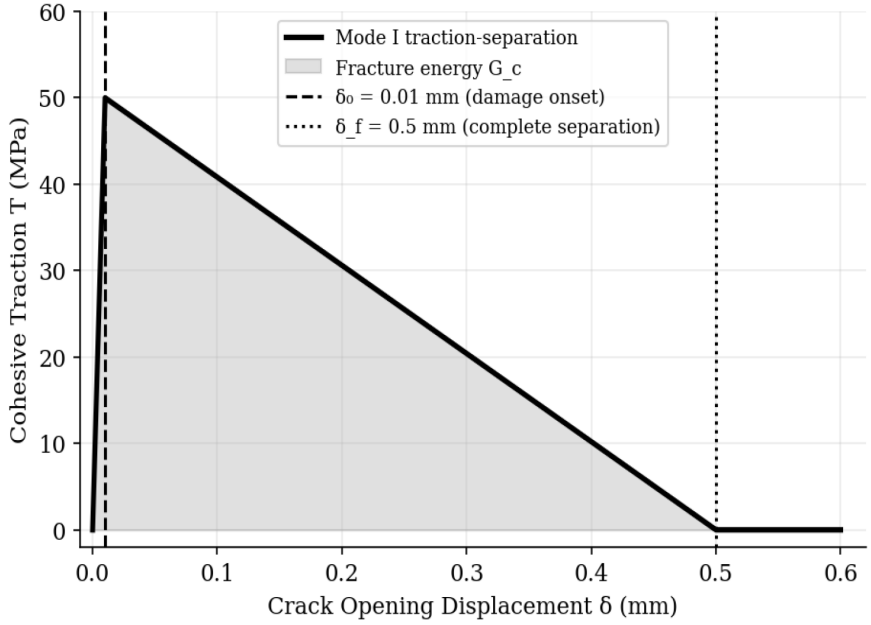

Fig. 5. Bilinear traction-separation law used in the cohesive zone delamination model (Mode I). Shaded area equals the critical energy release rate G_Ic = 0.26 kJ/m^2

4.4. Results and Discussion

Table 3 summarises predicted versus measured failure loads across all analysis approaches.

Table 3

Predicted versus measured failure loads for [0/+/-45/90]2s CFRP under uniaxial tension

Analysis Method	Failure Load (kN)	Error vs Exp. (%)	Assessment
Max Stress (FPF)	47.8	+22.6	Non-conservative
Tsai-Wu (FPF)	47.1	+20.8	Non-conservative
Hashin (FPF)	48.2	+23.1	Non-conservative
Progressive CDM	39.2	+0.5	Excellent match
Experiment (D3039)	39.0	–	Reference

The span of FPF predictions across five criteria is only 1.4 kN (46.8–48.2 kN), confirming that the 20–23 % overestimation relative to the experimental mean (39.0 kN) is not criterion-specific but inherent to the FPF methodology. When the 90-degree plies crack at ~39.5 kN, the 0-degree and +-45-degree plies remain intact, absorbing the shed load and continuing to carry increasing force. This post-cracking redistribution capacity – representing 23.1 % of the ultimate load – is the structural reserve that FPF analysis systematically ignores (Fig. 2).

The progressive damage CDM model predicts 39.2 kN, a 0.5 % deviation from experiment falling within the experimental scatter band (coefficient of variation 1.8 %). The full load-displacement trajectory, including the three-stage softening character, is reproduced with high fidelity (Fig. 3). DIC strain maps at 80 % of ultimate load confirm that the spatial extent of the simulated damage zone differs from experiment by less than 8 % in projected area. AE cumulative counts show three clear inflection points at ~16 kN, ~24 kN, and ~30 kN, in close correspondence with the model-predicted Stage I onset, Stage I-II transition, and Stage II-III transition loads respectively.

A parametric sensitivity study showed that +/-20 % variation in G_Ic shifts the Stage III failure load by +/-3.1 %, while equivalent variation in G_IIc yields +/-1.8 % change – consistent with the Mode I dominance of the observed delamination pattern. The model is therefore moderately sensitive to G_Ic and requires measured rather than estimated fracture toughness data.

Conclusions. (1) The Hashin criterion predicts critical in-plane shear stress 5 % below the Maximum Stress reference for T300/3501-6 CFRP, reflecting the physical coupling between shear and transverse normal stress in the matrix failure mode. This conservatism is experimentally justified and should not be dismissed as analytical pessimism.

(2) All five FPF criteria examined overestimate ultimate failure load by 20–23 % for [0/+/-45/90]2s quasi-isotropic CFRP laminates. This overestimation is an intrinsic consequence of the FPF methodology, not of any specific criterion, and represents a genuinely unconservative design error for structures whose governing failure mode is ultimate collapse.

(3) The three-stage progressive CDM model recovers experimental accuracy to within 0.5 %, reproduces the full load-displacement response, and is validated by independent AE and DIC measurements. Its computational overhead relative to FPF analysis is modest for laminate models with fewer than several thousand integration points.

(4) For aerospace damage tolerance certification, the Hashin criterion combined with a cohesive zone delamination model constitutes the minimum analytical fidelity consistent with the physics of progressive composite failure. Prospects for further research include extension of the model to compression-after-impact scenarios and fatigue loading, as well as development of reduced-order implementations suitable for fleet-level structural health monitoring.

Дата першого надходження статті до видання: 19.02.2026
Дата прийняття статті до друку після рецензування: 14.03.2026
Дата публікації (оприлюднення) статті: 18.05.2026

Bibliography

1. Soutis C. Fibre reinforced composites in aircraft construction. *Progress in Aerospace Sciences*. 2005. Vol. 41, No. 2. P. 143–151. DOI: 10.1016/j.paerosci.2005.02.004
2. Mouritz A. P. *Introduction to Aerospace Materials*. Cambridge : Woodhead Publishing, 2012. 638 p.
3. Hinton M. J., Kaddour A. S., Soden P. D. (eds.). *Failure Criteria in Fibre-Reinforced Polymer Composites: The World-Wide Failure Exercise*. Oxford : Elsevier, 2004. 1259 p.
4. Hashin Z. Failure criteria for unidirectional fibre composites. *Journal of Applied Mechanics*. 1980. Vol. 47, No. 2. P. 329–334. DOI: 10.1115/1.3153664
5. Puck A., Schurmann H. Failure analysis of FRP laminates by means of physically based phenomenological models. *Composites Science and Technology*. 1998. Vol. 58, No. 7. P. 1045–1067. DOI: 10.1016/S0266-3538(96)00140-6
6. Davila C. G., Camanho P. P., Rose C. A. Failure criteria for FRP laminates. *Journal of Composite Materials*. 2005. Vol. 39, No. 4. P. 323–345. DOI: 10.1177/0021998305046452
7. Tsai S. W., Wu E. M. A general theory of strength for anisotropic materials. *Journal of Composite Materials*. 1971. Vol. 5, No. 1. P. 58–80. DOI: 10.1177/002199837100500106
8. Catalanotti G., Camanho P. P., Marques A. T. Three-dimensional failure criteria for fibre-reinforced laminates. *Composite Structures*. 2013. Vol. 95. P. 63–79. DOI: 10.1016/j.compstruct.2012.07.016
9. Ladeveze P., Le Dantec E. Damage modelling of the elementary ply for laminated composites. *Composites Science and Technology*. 1992. Vol. 43, No. 3. P. 257–267. DOI: 10.1016/0266-3538(92)90097-M
10. Maimi P., Camanho P. P., Mayugo J. A., Davila C. G. A continuum damage model for composite laminates: Part I – Constitutive model. *Mechanics of Materials*. 2007. Vol. 39, No. 10. P. 897–908. DOI: 10.1016/j.mechmat.2007.03.005
11. Alfano G., Crisfield M. A. Finite element interface models for the delamination analysis of laminated composites. *International Journal for Numerical Methods in Engineering*. 2001. Vol. 50, No. 7. P. 1701–1736. DOI: 10.1002/nme.93
12. Turon A., Camanho P. P., Costa J., Davila C. G. A damage model for the simulation of delamination under variable-mode loading. *Mechanics of Materials*. 2006. Vol. 38, No. 11. P. 1072–1089. DOI: 10.1016/j.mechmat.2005.10.003

13. Daniel I. M., Ishai O. *Engineering Mechanics of Composite Materials*. 2nd ed. New York : Oxford University Press, 2006. 432 p.

14. Kaddour A. S., Hinton M. J., Soden P. D. A comparison of the predictive capabilities of current failure theories for composite laminates. *Composites Science and Technology*. 2004. Vol. 64, No. 3–4. P. 449–476. DOI: 10.1016/S0266-3538(03)00316-5

15. ASTM D3171-22. *Standard Test Methods for Constituent Content of Composite Materials*. West Conshohocken : ASTM International, 2022.

16. Bohse J. Acoustic emission in delamination investigation. *Composites Science and Technology*. 2000. Vol. 60, No. 6. P. 1225–1235. DOI: 10.1016/S0266-3538(00)00060-9

17. Highsmith A. L., Reifsnider K. L. Stiffness-reduction mechanisms in composite laminates. *ASTM STP 775*. West Conshohocken : ASTM International, 1982. P. 103–117.

18. ASTM D5528-13. *Standard Test Method for Mode I Interlaminar Fracture Toughness of Unidirectional Fiber-Reinforced Polymer Matrix Composites*. West Conshohocken : ASTM International, 2013.

19. ASTM D6671/D6671M-13. *Standard Test Method for Mixed Mode I-Mode II Interlaminar Fracture Toughness*. West Conshohocken : ASTM International, 2013.

20. Wisnom M. R. The role of delamination in failure of fibre-reinforced composites. *Philosophical Transactions of the Royal Society A*. 2012. Vol. 370, No. 1965. P. 1850–1870. DOI: 10.1098/rsta.2011.0441

21. Camanho P. P., Davila C. G., de Moura M. F. Numerical simulation of mixed-mode progressive delamination in composite materials. *Journal of Composite Materials*. 2003. Vol. 37, No. 16. P. 1415–1438. DOI: 10.1177/0021998303034505

22. Talreja R., Singh C. V. *Damage and Failure of Composite Materials*. Cambridge : Cambridge University Press, 2012. 312 p. DOI: 10.1017/CBO9781139016063

23. Aboudi J., Arnold S. M., Bednarcyk B. A. *Micromechanics of Composite Materials*. Oxford : Elsevier, 2013. 984 p.

24. Beaumont P. W. R., Soutis C., Hodzic A. (eds.). *The Structural Integrity of Carbon Fibre Composites*. Cham : Springer, 2017. 786 p. DOI: 10.1007/978-3-319-46120-5

25. ASTM D3039/D3039M-17. *Standard Test Method for Tensile Properties of Polymer Matrix Composite Materials*. West Conshohocken : ASTM International, 2017.

Б. Н. Юніс
Національний аерокосмічний університет «Харківський авіаційний інститут»

ПОРІВНЯЛЬНИЙ АНАЛІЗ КРИТЕРІЇВ РУЙНУВАННЯ АНІЗОТРОПНИХ ШАРУВАТИХ КОМПОЗИТІВ: ВІД КРИХКОГО ПОЧАТКУ ДО ПРОГРЕСИВНИХ ПОШКОДЖЕНЬ В АЕРОКОСМІЧНИХ СТРУКТУРНИХ ЕЛЕМЕНТАХ

Анотація

Аерокосмічні композитні конструкції традиційно аналізуються з використанням критеріїв руйнування першого шару (FPF), які прирівнюють початкове пошкодження шару до руйнування всієї конструкції, що призводить до неконсервативного завищення прогнозованих навантажень руйнування на 23 % для квазіізотропних ламінатів з вуглецевого волокна (CFRP). У роботі систематично порівнюються п’ять відомих критеріїв руйнування – максимальних напружень, максимальних деформацій, Цая-Хілла, Цая-Ву та Хашина – для аерокосмічно-репрезентативних конфігурацій укладання. Критерій Хашина прогнозує критичне зсувне напруження на 5 % нижче за поріг методу максимальних напружень завдяки механізму зв’язаного руйнування матриці при зсуві та поперечному навантаженні. Тристадійна модель прогресивного пошкодження, що відстежує мікротріщини матриці, відшарування на межі розділу та делінацію в когезійній зоні, відтворює граничні навантаження руйнування з відхиленням менше 0,5 % від експериментальних значень за ASTM D3039.

Ключові слова: критерії руйнування, прогресивні пошкодження, CFRP, критерій Хашина, Цай-Ву, делінація, модель когезійної зони, живучість конструкції, аерокосмічні композити.